Uric Acid Enhances Neurogenesis in a Parkinsonian Model by Remodeling Mitochondria

Ji Eun Lee
Yonsei University College of Medicine, Seoul
Yu Jin Shin
Yonsei University College of Medicine, Seoul
Ha Na Kim
Yonsei University College of Medicine, Seoul
Dong Yeol Kim
Yonsei University College of Medicine, Seoul
Seok Jong Chung
Yongin Severance Hospital, Yonsei University Health System, Yongin
Han Soo Yoo
Yonsei University College of Medicine, Seoul
Jin Young Shin
Severance Biomedical Science Institute, Yonsei University, Seoul
Phil Hyu Lee (phlee@yuhs.ac)
Yonsei University College of Medicine, Seoul

Research Article

Keywords: Uric acid, Neurogenesis, Mitochondrial dynamics, Parkinson's disease

Posted Date: June 23rd, 2021

DOI: https://doi.org/10.21203/rs.3.rs-598298/v1

Abstract

Adult neurogenesis is the process of generating new neurons to enter neural circuits and differentiate into functional neurons. However, it is significantly reduced in Parkinson's disease (PD). Restoring neurogenesis is suggested to be a potential disease-modifying strategy to treat PD. Uric acid (UA), a natural antioxidant, has neuroprotective properties in patients with PD. Here, we hypothesized that UA would enhance neurogenesis by modulating mitochondria, dynamic organelles and key regulators of the fate of neural stem cells. We evaluated whether elevating serum UA levels in a 1-methyl-4-phenyl-1,2,3,6-tetrahydropyridine (MPTP)-induced parkinsonian model would restore neurogenesis in the subventricular zone (SVZ). UA-elevating therapy significantly increased the number of bromodeoxyuridine (BrdU)-positive cells in the SVZ of PD animals as compared to PD mice with normal UA levels. In a cellular model, UA treatment promoted cell proliferation against 1-methyl-4-phenylpyridinium (MPP^+) in primary cultured neural precursor cells (NPCs) from the SVZ. These findings demonstrate that UA enhances neurogenesis by modulating mitochondrial dynamics in the SVZ of parkinsonian models, suggesting UA elevating strategy as a potential disease-modifying therapy in treatment of parkinsonian disorders.

Introduction

Neurogenesis is the ability of the brain to produce neurons and strengthen existing connections between neuronal cells across the lifespan. Remarkably, the brain continually generates new neurons even after embryonic development. Under normal physiology, new neurons are generated from neural stem cells (NSCs) of the subventricular zone (SVZ) or subgranular zone, which then migrate to the neurogenesis niche, enter neural circuits, and differentiate into functional neurons [1]. This process is known to be involved in various brain functions such as memory formation, motor control, neuronal plasticity, and endogenous recovery. Ample evidence has demonstrated that patients with neurodegenerative diseases such as Alzheimer's disease, Parkinson's disease (PD), and Huntington's disease show deficient neurogenesis compared to healthy controls [2–4]. Gradual loss of neuronal populations and diseased neurons disrupt synaptic transmission, cell renewal, and putative function in neurodegenerative diseases [5]. Thus, restoring adult neurogenesis is considered to be one of the important strategies for treating patients suffering from neurodegenerative diseases [6].

PD is characterized by the selective loss of dopaminergic neurons in the substantia nigra (SN) and the degeneration of projecting nerve fibers to the striatum, leading to parkinsonian motor symptoms such as bradykinesia, rigidity, and tremor [7]. Among the multiple factors underlying PD pathogenesis, oxidative stress plays a key role in PD pathology via disrupting the electron transport chain and subsequent electron leakage from donor redox to molecular oxygen [8]. Moreover, oxidative stress is interwined with other mechanisms implicated in PD, including protein misfolding and aggregation, mitochondrial dysfunction, and apoptosis. Uric acid (UA), purine metabolite, is a powerful antioxidant, present intracellularly and in all body fluids. It not only scavenges reactive oxygen species (ROS) but also blocks the reaction of superoxide anion with nitric oxide that can injure cells by nitrosylating the tyrosine

residues of proteins, and prevents extracellular superoxide dismutase degradation [9]. Several epidemiological studies reported that UA has neuroprotective properties against PD, showing that PD patients with higher UA have reduced risk of PD incidence as well as slower disease progression [10,11]. Additionally, the beneficial effects of UA have been observed in other neurodegenerative diseases, such as amyotrophic lateral sclerosis [12], Alzheimer's disease [13], Huntington's disease [14], or other disorders [15,16]. These studies imply that in addition to antioxidant properties, UA may have another pathway to exerting neuroprotective effects against neurodegenerative conditions.

Emerging evidence indicates that mitochondria are central regulators of NSC fate decisions and are crucial for adult neurogenesis [17]. NSCs are not only dependent on generation of mitochondrial metabolites [18], but are also dependent on changes in mitochondrial morphology and metabolic properties across various stages of differentiation [19]. Mitochondrial malfunction makes stem cells vulnerable to oxidative stress, which in turn accelerates NSC death, resulting in reduced neurogenesis [20]. As mitochondria are dynamic organelles that change their size and morphology actively, the processes of fission and fusion oppose each other and allow the mitochondria to constantly remodel themselves depending on their environment [21,22]. A recent study found that adult neurogenesis in the hippocampus is critically dependent on mitochondrial complex function in mice and NSCs isolated from mice with malfunctioning mitochondria [23]. Indeed, mitochondrial dynamics may have an important role in neurogenesis via maintaining a functional mitochondrial network during biogenesis [24–26]. In this study, we hypothesized that UA would enhance neurogenesis by controlling mitochondrial dynamics in PD. To do this, we evaluated whether high levels of UA increase neurogenic activity in primary cultured neural precursor cells (NPCs) and SVZ of 1-methyl-4-phenyl-1,2,3,6-tetrahydropyridine (MPTP)-treated animals. In addition, we examined possible role of mitochondrial dynamics in UA-mediated modulation of neurogenesis in PD models.

Results

2.1. UA-elevating therapy increased neurogenesis in the SVZ of MPTP-induced PD animal model

To determine the effect UA elevation on neurogenesis in an MPTP-induced parkinsonian model, the mice were treated with uricase inhibitor (oxonate potassium, KOx) or UA precursor (inosine 5'-monophosphate, IMP) before MPTP treatment. Two weeks of KOx injection (500 mg/kg) slightly but not significantly raised the level of serum UA (88.3 g/L vs 85.8 g/L). However, 2 weeks of co-treatment of IMP (500 mg/kg) with KOx (250 mg/kg) led to a significant increase in the level of UA (76.4 g/L) relative to baseline (63.1 g/L, $p = 0.006$, Fig. 1B). To investigate whether UA-elevating therapy modulated neurogenesis, NPCs in the SVZ of mice were immunostained with BrdU, a commonly used marker for neurogenesis [27]. Compared to the control group, the number of BrdU-positive cells in ependymal and rostral migratory stream (RMS) was significantly reduced in the MPTP-treated mice by 46.2% ($p = 0.001$,

Fig. 1C-D). Compared to MPTP-only-treated mice, PD mice received co-treatment of IMP with KOx exhibited a significant increase in the number of BrdU-positive cells, restoring up to 85.3% ($p = 0.006$, Fig. 1C-D). Next, as dopaminergic neurons can modulate neurogenic activity via dopaminergic receptors in the SVZ, we determined whether UA elevation in MPTP-treated mice would lead to a difference in the density of nigral dopaminergic neurons. As expected, the number of TH (tyrosine hydroxylase)-positive cells in the SN was reduced to 51.5% in MPTP-treated animals compared to the control group ($p < 0.01$, Fig. 1C-D). However, the number of TH-positive cells in PD mice co-treated with IMP and KOx was not statistically different from the MPTP-only-treated group. We also investigated neurogenesis in hippocampal dentate gyrus (DG). MPTP induced PD mice showed decreased number of BrdU positive cells in DG by 19.1% compared to control group ($p < 0.001$, Supplementary Fig. 1A, 1B). Compared to MPTP-treated mice, PD mice received UA elevating therapy showed significantly increased number of BrdU-positive cells ($p < 0.001$, Supplementary Fig. 1A, 1B).

These data indicate that UA-elevating therapy promotes neurogenic activity in MPTP-induced parkinsonian animals without modulating the nigrostriatal dopaminergic system.

2.2. UA treatment exerted a neuroprotective effect and enhanced proliferation against MPP^+ in primary cultured NPCs from the SVZ

Primary cultured NPCs were positive for nestin, sox2, doublecortin, and musashi, but negative for GFAP (data not shown). To examine the effect of UA on cell survival followed by MPP^+ treatment, primary cultured NPCs were treated with MPP^+ at various concentrations for 72 h. MPP^+ treatment with a concentration of 150 μM or more markedly decreased cell viability of NPCs in a dose-dependent manner (Fig. 2A). However, UA treatment at various concentrations did not result in decreased viability of NPCs (Fig. 2B). Next, we examined if UA treatment exhibited a neuroprotective effect against MPP^+-induced cytotoxicity in NPCs. Similar to *in vivo* data, UA treatment in MPP^+-treated NPCs exerted a prosurvival effect, restoring cell viability up to 90.1% compared to the MPP^+-treated group ($p = 0.049$, Fig. 2C). On evaluating proliferation of NPCs, the mRNA expression level of Ki67 was significantly decreased in MPP^+-treated NPCs, whereas UA treatment markedly increased the level of Ki67 relative to the MPP^+ treatment group ($p = 0.026$, Fig. 2D). Similarly, UA treatment significantly increased the protein level of Ki67 compared to the MPP^+ treatment group (Fig. 2F, 2G). We also measured intracellular ROS level in NPCs. As expected, MPP^+ treatment increased ROS level compared to controls ($p = 0.023$, Fig. 2E). However, when UA was treated prior to MPP^+ treatment for 24 h, it significantly scavenged excessive ROS, restoring back to control level ($p = 0.047$, Fig. 2E). These data suggest that UA not only increased the survival of NPCs against MPP^+ toxicity, but also enhanced proliferation *in vitro.* Next, the modulatory mechanism of UA on neurogenic activity was further studied in mitochondrial dynamics. Immunofluorescent labeling for mitotracker showed that MPP^+-treated NPCs displayed many more fragmented mitochondria rather than tubular shape. Whereas, UA treated NPCs exhibited more interconnected, elongated and filamentous mitochondria similar to those of naïve NPCs (Fig. 2H). These data imply that when NPCs are exposed to

MPP^+, their mitochondria go through a fission process. However, UA treatment has scavenged MPP^+ toxin, promoting fusion machinery and inhibiting fission process.

2.3. UA treatment rescued the abnormal mitochondrial phenotype observed in primary cultured NPCs by modulating mitochondrial dynamics.

To investigate the mitochondrial dynamics modulatory mechanism in detail, mitochondrial dynamics-related genes were measured with quantitative real-time PCR analysis. Under MPP^+ treatment, mitochondrial master regulator, PGC-1α, tended to decrease in NPCs but did not reach statistical significance ($p = 0.406$), whereas UA treatment significantly upregulated the expression of PGC-1α compared to the only-MPP^+-treated group ($p = 0.029$, Fig. 3A). The expression level of fission marker, Fis1, was markedly increased in NPCs approximately two-fold following MPP^+ treatment ($p = 0.021$); however, UA treatment counteracted the expression of Fis1 in MPP^+-treated NPCs. Conversely, mitochondrial fusion marker, Mfn2, was significantly decreased in NPCs following MPP^+ treatment as compared to the control group ($p = 0.093$), whereas UA treatment restored the expression of Mfn2 in MPP^+-treated NPCs ($p = 0.011$).

In addition, UA treatment in MPP^+-treated NPCs significantly increased the expression of mitochondrial transcription factor, Tfam ($p = 0.001$) relative to the MPP^+-treated group. These data indicate that UA has scavenged MPP^+ toxins by modulating mitochondrial dynamics. Next, we evaluated the changes of actual mitochondrial morphology using TEM analysis. Mitochondrial morphology was preserved in control NPCs, with well-formed cristae and undisrupted mitochondria membranes. However, mitochondria following MPP^+ treatment were filled with discontinuous cristae, electron-dense structures, and damaged double-membranes. Additionally, mitochondria in MPP^+-treated NPCs exhibited swollen bodies (Fig. 3B). The TEM image data suggest that treatment of MPP^+ leads to mitochondrial damage, possibly triggering fission process and/or inhibiting fusion process. However, UA treatment successfully returned mitochondrial morphology to a healthy form, similar to those of naïve NPCs, through a possible rescue of mitochondrial dynamics balance of fusion and fission processes (Fig. 3B).

2.4. PD mice with elevated serum UA levels showed increased BrdU-positive cell numbers through modulation of mitochondrial dynamics key actors

Next, mitochondrial dynamics-related proteins were analyzed to investigate whether UA elevation could modulate mitochondrial dynamics in the SVZ of MPTP-treated animals. The protein expression of mitochondrial fusion marker, Mfn1, was significantly decreased in MPTP-treated animals as compared to control mice ($p = 0.034$), and another marker, Mfn2, was slightly decreased in the parkinsonian model as compared to healthy mice ($p = 0.519$). The expression of the inner membrane optic atrophy protein (OPA1) tended to decrease in MPTP-treated mice relative to control mice ($p = 0.318$, Fig. 4A). However, UA elevation in MPTP-treated animals led to an increase in the expression of Mfn1 ($p = 0.127$), Mfn2 ($p = 0.028$), and OPA1 ($p = 0.007$) as compared to the MPTP-only-treated group (Fig. 4A). Conversely, the

expression of mitochondrial fission-related protein, GTPase Dynamin-related protein 1 (Dlp1), was significantly increased in MPTP-treated animals compared to control animals ($p = 0.041$). Another fission regulator, Fis 1, was slightly increased in the parkinsonian model compared to healthy animals ($p = 0.506$). Meanwhile, UA elevation in MPTP-treated animals led to a significant increase in expression of Dlp1 and Fis1 ($p = 0.029$ and 0.002, respectively) compared to the MPTP-only-treated group (Fig. 4B). Finally, UA elevation led to a significant increase in expression of nestin in the SVZ of MPTP-treated animals ($p = 0.021$, Fig. 4C).

Discussion

This study aimed to investigate whether elevation of serum UA levels modulate neurogenic activity in a parkinsonian model. The major findings of present study are 1) UA elevation in MPTP-induced PD mice led to an increased number of BrdU-positive cells in the SVZ and DG compared to MPTP-only-treated mice. 2) UA treatment exerted a prosurvival effect, restoring viability and proliferation of NPCs against MPP^+ treatment. 3) In the process of modulating neurogenesis, our *in vitro and in vivo* data demonstrated that UA elevation regulated mitochondrial dynamics via promoting fusion machinery. The results suggest that UA enhances neurogenic activity in the SVZ of a parkinsonian model by modulating mitochondrial dynamics.

Although the underlying molecular mechanisms of the altered neurogenesis in PD remain unknown, neurochemical deficits of dopamine [28], indirect effects of growth factor release, and α-synuclein accumulation in NPCs of the SVZ via the disease process may influence neurogenic activity [29]. Several studies have demonstrated the effect of α-synuclein in the hippocampus and SVZ of transgenic animal models and murine embryonic stem cells [30–33]. In addition, recent evidence has demonstrated that mitochondrial dysfunction and inappropriate regulation of mitochondrial dynamics have detrimental effects on neurogenesis in the embryonic as well as adult brain. During neurogenesis, mitochondrial dysfunction resulting from deletion of the mitochondrial oxidoreductase protein AIF within the early NSC population disrupted the neurogenic pathway completely, including self-renewal capacity of NSC and proliferation and differentiation of NPCs [20]. Likewise, disruption of mitochondrial function by loss of the mitochondrial transcription factor, Tfam, when restricted to the adult NSC population, leads to impairment in adult neurogenesis. During embryonic neurogenesis, mitochondrial dynamics seem to play an important role in the stem cell decision-making process enhanced mitochondrial fusion promotes NSC self-renewal, while mitochondrial fragmentation initiates the commitment of NSC to neuronal differentiation and neuronal maturation [24]. A recent study reported that inhibition of mitochondrial fission improved mitochondrial dynamics and stimulated hippocampal neurogenesis in Down syndrome animal model [34]. Therefore, maintenance of proper mitochondrial dynamics would be an important strategy to modulate neurogenic activity in PD.

The present study has demonstrated that UA elevation in MPTP-induced PD mice led to an increased number of BrdU-positive cells in the SVZ compared to MPTP- only-treated mice, restoring up to 85% of

neurogenic activity compared to the control mice. In a cellular model using primary culture of NPCs, UA treatment exerted a prosurvival effect, restoring cell viability of NPCs against MPP^+ treatment and led to increased proliferation markers. As impairment in neurogenesis is known to be a critical factor in neurodegenerative diseases including PD, modulating it could be an effective strategy in disease-modifying treatment. Accumulating clinical data have also reported an association between high serum UA levels and lower likelihood of developing PD [35]. Furthermore, we found that the hippocampal neurogenesis was also enhanced with UA-elevating therapy. Previous studies have demonstrated that UA decreases the risk of dementia in general population mice [36] and improves cognitive performance in PD mice through the Nrf2-ARE signaling pathway [37]. Hence, it is possible that UA could improve cognitive function through modulation of hippocampal neurogenesis. A further research is warranted to investigate whether UA would be helpful in AD models by modulating hippocampal neurogenic activity.

Interestingly, we have demonstrated that UA may modulate neurogenesis by remodeling mitochondria. Mitochondria are dynamic organelles that constantly change their size and morphology in response to the environment in the machinery of fission and fusion. In mammals, Mfn1, Mfn2, and OPA1 are responsible for mitochondrial fusion, while Dlp1 and Fis1 are required for mitochondrial fission. Fission is a process of breaking apart into smaller fragments, which is important for segregating dysfunctional mitochondria from healthy counterparts [38]. Therefore, this process plays an important role in quality control of maintaining healthy mitochondria, further sustaining healthy neurons that require considerable energy. In the process of neurogenesis, a critical amount of ATP is required to facilitate cytoskeletal rearrangement, neuronal sprouting, and organelle transport. Being a primary source of cellular ATP, healthy mitochondrial function is necessary for the brain to perform neurogenesis effectively. In terms of the association between oxidative stress and neurogenesis, several studies have highlighted the fact that oxidative stress load directly affects cellular states by modulating the redox state of NSCs or NPCs, given that adult neurogenesis is a high-energy-consuming process, and thus, leads to ROS accumulation [39]. MPTP, the neurotoxin widely known to induce PD models, is highly lipophilic, and so it can rapidly cross the blood brain barrier after systemic administration. MPTP is metabolized within the brain to active toxin MPP^+ by monoamine oxidase, resulting in mitochondrial complex I dysfunction and impaired mitochondrial homeostasis [40]. Mitochondrial malfunction, already problematic in the process of PD, makes stem cells vulnerable to oxidative stress, which in turn accelerates impairment of neurogenesis. Moreover, emerging data from human and animal models of PD have reported that α-synuclein has an important role in the control of neuronal mitochondrial dynamic processes [41,42], suggesting a strong candidate for a pathogenic mechanism underpinning PD pathogenesis beyond mitochondrial biogenesis, a well-known factor. Therefore, UA, having potent antioxidant properties, would defend mitochondrial homeostasis and dynamics against MPTP-induced oxidative stress, which can lead to maintenance of neurogenic activity in the SVZ of PD models. Accordingly, our data provide additional evidence that modulation of neurogenic activity via a UA-elevating strategy may be an intriguing mechanism in the development of future PD treatments.

Recent studies have suggested the important role of dopaminergic modulation in the neurogenic activity of the SVZ by demonstrating that NPCs in the SVZ express dopaminergic receptors and dopaminergic innervation from the SN in a 6-OHDA-induced PD rat model [43,44]. Specifically, dopamine agonists augment neurogenesis in animal models of PD [45], and chronic use of levodopa has a positive effect on the number of NSCs in the SVZ of patients with PD [46]. Based on these previous data, the present study evaluated the density of nigral dopaminergic neurons between MPTP-induced PD animals with and without UA-elevating therapy to exclude the direct effect of nigral dopamine on neurogenesis in the SVZ. However, there was no significant change in nigral dopaminergic density between groups, suggesting that the modulating effect of UA on neurogenesis in NPCs of the SVZ may reflect a primary effect of UA itself rather than an indirect effect of dopaminergic medication.

This study has several limitations to extend clinical implications. First, although neuroprotective effect of UA in PD incidence and progression seems to be sex-dependent [47], the present study examined effect of UA elevation on neurogenic activity only in male PD mice. Further study of UA-mediated neurogenic activity in female animals is also necessary. Second, although serum UA levels increased following injection of IMP with KOx, post-treatment after MPTP induction without pre-treatment prior to MPTP induction did not lead to a significant increase in neurogenesis. In both an animal and cellular model, pre-treatment of UA enhanced neurogenesis and exerted prosurvival effect of NPCs. Regarding these data, neurogenic modulation of UA seems to be effective in the premotor stage of PD; however, this issue should be investigated in future studies. Third, due to lack of immunohistochemical data co-staining BrdU-positive cells with neuronal cells, the data regarding neurogenesis should be cautiously interpreted. Finally, we couldn't provide mitochondrial morphology in animal tissue with immuno-detection, which may limit the role of UA in mitochondrial dynamics.

In conclusion, this study demonstrates that UA elevation can enhance neurogenic activity in the NPCs of the SVZ in parkinsonian animal and cellular models by modulating mitochondrial dynamics. Our data suggest that a UA-elevating strategy may be a potential disease-modifying therapy for PD patients by enhancing neurogenesis.

Methods

4.1. Parkinsonian animal model and drugs administration

All procedures were performed in accordance with the Laboratory Animals Welfare Act, the Guide for the Care and Use of Laboratory Animals and the Guidelines and Policies. The rodent experiment was approved by IACUC (Institutional Animal Care and Use Committee) in the Yonsei University Health System (approval number: 2017 – 0238). ARRIVE guidelines were followed (http://arriveguidelines.org). Male C57BL/6J mice (4 weeks old) were acclimated in a climate-controlled room with a constant 12 h light/dark cycle (12 h on, 12 h off) for a week prior to the initiation of drug administration. At 5 weeks of age, the mice were randomly divided into three groups: control group, MPTP PD group, and MPTP PD + UA treatment group. To elevate serum UA levels, UA treatment group mice received an i.p injection of

potassium oxonate (Sigma, 500mg/kg; KOx) and inosinic acid (Sigma, 500mg/kg; IMP) daily for 2 weeks while others received normal saline. To construct parkinsonian model, the mice (except for those in the control group) received a sub-acute injection of MPTP freshly dissolved in 20% DMSO/ 80% normal saline (25mg/kg) by i.p injection (Sigma, St. Louis, MO, USA) for 5 days. After 72 h had passed since the last MPTP injection, UA groups received 4 weeks of UA injections. Four days prior to last UA injection, all animals received a bromodeoxyuridine (BrdU) injection (Sigma, 100mg/kg) daily on 5 consecutive days. The in vivo study design is illustrated in Fig. 1.

4.2. Preparation of serum and brain tissue

At the end of the experimental period, mice were deeply anesthetized with isoflurane and their blood and brains were collected. To evaluate whether serum UA levels were elevated by injection of KOx and IMP, mouse blood samples were collected in SST tubes (BD Diagnostic Systems, Sparks, MD, USA), and serum and blood cells were separated by centrifugation (2000 × g for 20 min). The isolated serum samples were rapidly frozen and stored at -20°C until analyzed. For immunohistochemistry, the mice were perfused with 4% paraformaldehyde. Brains were harvested from the skulls, post-fixed overnight in 4% paraformaldehyde, and stored in 30% sucrose solution for 1–2 days at 4℃ until they sank. Finally, 25-μm coronal sections were obtained using cryostat. The sections were stored in tissue storage solution (30% glycerol, 30% ethylene glycol, 30% distilled water, 10% 0.2M PB) at 4℃ until required [48].

4.3. NPC primary culture and identification

NPCs were isolated from a postnatal day-1 Sprague-Dawley rat. Offspring of rats were decapitated under halothane anesthesia. Brain tissue was taken from the rat and a wedge of tissue was microdissected from the portion of the lateral ventricle that included the anterior part of the SVZ. The tissues were incubated in Hank's balanced salt solution (HBSS) for 10min and trypsin for 3min at room temperature. NPCs were dissociated into single cells by pipetting, and Dulbecco's modified eagle medium (DMEM) supplementation with 10% fetal bovine serum (FBS; Hyclone) and 1% penicillin/streptomycin (P/S; Hyclone) was added to inhibit trypsin function. Cells were plated in 100-mm plastic culture dishes and cultivated in low glucose DMEM in a humidified incubator at 37°C under 5% CO_2. After 24 h, non-adherent cells were removed by changing media. To identify characteristics of NPCs, total RNA was extracted from the NPCs using Trizol reagent (Lugen Sci, Korea) according to the manufacturer's instructions. RNA concentration was measured by absorption at 260 nm using NanoDrop Lite Spectrophotometer (Thermo Scientific, Wilmington, DE, USA) and an equal amount of RNA (approximately 1ug) in each experiment was reverse transcribed. The PCR reaction was performed using 10pmol each of the primers for Nestin (forward 5'-GGCCACAGTGCCTAGTTCTT-3', reverse 5'-GTTCCCAGATTTGCCCCTCA), Sox2 (forward 5'-TAAGTACACGCTTCCCGGAG-3', reverse 5'-CATCATGCTGTAGCTGCCGT-3'), Doublecortin (forward 5'-TCACAGCATCTCCACCCAAC-3', reverse 5'-ATGCCTGCAAGGTTCTGGTT-3'), Musashi1 (forward 5'-CGGAGAGCACAGCCTAAGAT-3', reverse 5'-TCGAACGTGACAAACCCGAA-3'), and GFAP (forward 5'-ACGAGGCTAATGACTATCGC-3', reverse 5'-GTTTCTCGGATCTGGAGGTT-3'). After an initial denaturation at 95℃ for 10 min, 30 cycles of PCR were performed, consisting of denaturation at 95℃ for 20 s, annealing at 60℃ for 30 sec, extension at 72℃ for 60 s followed by a final extension at 72℃ for 5 min. The PCR

products were separated by electrophoresis on 1.5% agarose gel and stained with Noble View (Noble Bio). Gels were examined under UV illumination Gel doc (MiniBISpro, DNR).

4.4. NPC treatment

Identified NPCs (positive for nestin, sox2, doublecortin, and musashi, but negative for GFAP)

were seeded in 96-well cell culture plates (SPL) at a density of 0.5×10^4/well. Plates were incubated at 37℃ for 72 h to allow cells to be attached. Solution of MPP^+ and UA were prepared in advance. MPP^+ (sigma) was dissolved in distilled water to a final concentration of 100mM stock. After stabilization, each well was randomly divided into three groups as follows: control group, MPP^+ group, MPP^+/UA group. MPP^+/UA group cells were treated with 150 μM of UA while others were just changed media. After 24 h, MPP^+ group was treated with 150 μM of MPP^+ and UA group was treated with 150 μM of MPP^+ and UA mixture. Plates were incubated in a cell incubator for 72 h. 150 μM of MPP^+ was treated to the MPP^+ group cells and the MPP^+ and UA mixture were treated to both UA groups. Plates were incubated in a cell incubator for an additional 72 h.

4.5. Cell viability analysis

Cell viability was measured by MTS cell proliferation assay (promega). According to the assay manufacturer's instructions, right before the measurement time, MTS and PMS were mixed in a 1 ml:50 μl ratio and incubated for 10 min. Then, 20 μl of mix was added to each well. The plates were incubated at 37℃ for 1 h, and we measured the absorbance at 490 nm using a 96-well plate reader. Cell viability values were expressed as experimental group / average of control group x 100 = viability percentage. All experiments were repeated at least three times.

4.6. Measurements of serum UA level

Serum UA levels were measured using an Amplex Red Uric Acid/Uricase Assay Kit (Molecular Probes, Eugene, OR) according to the manufacturer's instructions. Each serum samples were 1/10 diluted for measurement. Briefly, uricase catalyzes the conversion of UA to allantoin, H_2O_2, and CO_2. Under the presence of horseradish peroxidase, H_2O_2 reacts stochiometrically with Amplex Red reagent to generate the red-fluorescent oxidation product, resorufin, which is measured using excitation at 540 nm and detection at 590 nm.

4.7. Measurements of ROS level

The level of intracellular ROS in NPCs was measured using 2', 7'-Dichlorofluorescin diacetate (DCFDA), DCFDA Cellular ROS Detection Assay Kit (ab113851, Abcam, UK). This reagent diffuses into the cell, which goes through deacetylation and oxidization by cellular enzymes into 2',7'-dichlorofluorescein (DCF). According to manufacturer's protocol, cells were seeded at $1x10^4$ cells/well in 96well plate. When chemical treatment was done, cells were washed twice with 1X buffer. Washed cells were incubated with 25μM DCFDA solution for 45 min at 37℃. Then, DCFDA solution was removed, cells were washed with buffer again, and the level of ROS was measured using excitation at 485 nm and detection at 535 nm.

4.8. Immunohistochemistry

When drug administration was done in the animal model, brain tissue was immunostained with BrdU and TH (1:500, Sigma, St. Louis, MO, USA) in SVZ and SN respectively to investigate newborn neurons and dopaminergic neurons, which we interpret as the degree of neurogenesis and as confirmation of the MPTP parkinsonian model. First, brain tissues were frozen with O.C.T. compound (Sakura Finetek) and 25-um coronal sections were obtained using cryostat. Sections were immunostained using immunofluorescence analysis or 3,3-diaminobenzidine (DAB) method. For BrdU detection, the slides were washed three times in PBS, incubated with 50% formamide in 2X SSC DW (standard saline citrate distilled water) for 2h at 65℃ for antigen retrieval, and rinsed three times in 2X SSC DW. After rinsing, the slides were incubated with 2N HCl in DW for 30min at 37℃ to denature DNA and rinsed three times in PBS. They were incubated in borate buffer (0.1 M, pH-8.5) to neutralize the acidic medium and then blocked in 3% H_2O_2 to remove endogenous peroxidase for 10min. To reduce nonspecific binding, slides were blocked with 1% BSA in PBST for 2 h at room temperature and incubated with primary antibody, mouse anti-BrdU (1:500, Thermofisher Scientific, Waltham, MA, USA) for overnight at 4℃. The antibody was detected with 0.05% diaminobenzidine (DAB, Dako, Carpinteria, CA). Immunofluorescence labeling was carried out by incubating tissue slides in donkey anti-mouse IgG and goat anti-rabbit IgG (both Alexa Fluor-488, green and Alexa Fluor-555, red) secondary antibodies (1:200, invitrogen). The cell nuclei were counterstained with 4’,6-diamidino-2-phenylindole (DAPI; 1:2000 dilution, invitrogen). The brain tissue was dried and stained with Mayer’s hematoxylin (Muto Pure Chemicals Ltd., Tokyo, Japan). The immunostained tissues were analyzed using bright-field microscopy and immunofluorescence images were viewed with a Zeiss LSM 700 confocal microscope (Carl Zeiss, Berlin, Germany) [49].

4.9. Quantitative real-time PCR

Total RNA was isolated from NPCs using Trizol reagent (Lugen Scei, Korea) according to manufacturer’s instructions. An equal amount of RNA (approximately 1 ug) in each experiment was reverse transcribed using an cDNA synthesis premix. A master mix of the following reaction components was prepared to the indicated end-concentration: 12.5 µl of 2X SYBR green buffer, 2 µl of forward and reverse primer (10 pM), and 2 µl DNA template (100 ng). Amplification conditions were as follows: initial denaturation at 95℃ for 2min, followed by 40 amplification cycles of 95℃ for 15s and 60℃ for 1 min to anneal and extend, respectively. Quantitative PCR experiments were performed using Applied Biosystems (Thermofisher Scientific, Waltham, MA, USA). The quantitative real-time PCR reaction was performed using 10pmol each of the primers for rat PGC1-α (forward 5’-GGACATGTGCAGCCAAGACT-3’, reverse 5’-TCGAATATGTTCGCGGGCTC), Fis1 (forward 5’-CGTGCTTTCTGTAACGCCTG-3’, reverse 5’-CTACAGGCACTTTGGGGGTT-3’), Mfn2 (forward 5’-AAGAGCTCAGGGGACGGTAT-3’, reverse 5’-GCAAGGTGAGCCTTACAGGT-3’), and Tfam (forward 5’-GTGATCTCATCCGTCGCAGT-3’, reverse 5’-CATTCAGTGGGCAGAAGTCCA-3’) [50].

4.10. MitoTracker staining

To visualize mitochondria, MitoTrackerRed CMXRos (Invitrogen, Camarillo, CA, USA) was diluted in NPC cell culture media to a final concentration of 50 nM according to manufacturer's instructions. The cells were incubated under normal culture conditions for 30 min, fixed with 1:1 ratio of methanol and acetone for 5 min at -20℃, and permiabilized with 0.1% triton X-100 in PBS. All NPCs were counter stained for nuclei using DAPI (blue), and then visualized by a Zeiss LSM 700 confocal microscope (Carl Zeiss, Berlin, Germany) and Zen imaging software. All cells were imaged using identical exposure times and laser power settings.

4.11. EM analysis

Primary cultured NPCs were fixed with 2% glutaraldehyde - paraformaldehyde in 0.1 M PB (pH 7.4) for 12 h and then washed twice for 30 min in 0.1 M PB. They were post-fixed with 1% OsO4 dissolved in 0.1 M PB for 2 h and dehydrated in an ascending gradual series (50 to 100%) of ethanol and infiltrated with propylene oxide. Specimens were embedded using a Poly/Bed 812 kit (Polysciences). After pure fresh resin embedding and polymerization at 65°C in an electron microscope oven (TD-700, DOSAKA) for 24 h, 200nm- thick sections were initially cut and stained with toluidine blue for light microscopy. Thin sections (80 nm) were double stained with 3% uranyl acetate and lead citrate for contrast staining. The sections were cut using a Leica EM UC7 Ultra-microtome (Leica Microsystems). All of the thin sections were observed by transmission electron microscopy (JEM-1011, JEOL) at an acceleration voltage of 80 kV.

4.12. Western blotting analysis

When animal drug administration was over, half of the mice in each group were fixed with paraformaldehyde while the rest of their SVZ was dissected under a microscope, and then total protein was extracted. Brain tissues were dissolved in ice-cold RIPA buffer (50 mM Tris-HCl, pH 7.5, with 150 mM sodium chloride, 1% triton X-100, 1% sodium deoxycholate, 0.1% SDS, 2 mM EDTA sterile solution; Lugen Sci, Korea) plus protease inhibitor cocktail (Sigma). The lysates were centrifuged at 4℃ for 20 min (14,000 g), and supernatants were transferred to fresh tubes. Briefly, 30ug of protein was separated by SDS-gel electrophoresis and transferred to hydrophobic polyvinylidene difluoride (PVDF) membranes (GE Healthcare, Little Chalfont, UK). The membranes were blocked in 5% skim milk in PBST. Membranes were probed with the following primary antibodies: mouse anti-Mfn1 (Abcam), rabbit anti-Mfn2 (Epitomics), mouse anti-OPA1 (BD biosciences), rabbit anti-Fis1 (Abnova), mouse anti-Dlp1 (BD biosciences), mouse anti-nestin (Millipore), and mouse anti-Actin (santacruz). As secondary antibodies, 1:5000 dilutions of horseradish peroxidase-conjugated goat anti-rabbit antibody (Solarbio) and anti-mouse antibody (Solarbio) were used. Antigen–antibody complexes were visualized with ECL solution (GenDEPOT). For quantitative analysis, immunoblotting band densities were measured by image J [50].

4.13. Stereological cell counts

To determine the number of BrdU- and TH-positive cells in the granule cell layer of mouse brains, an average of five sections per mouse were counted, and each experimental group consisted of five mice. All

of the counting was performed under a microscope using a 40x objective in stacks of five optical sections.

4.14. Statistical analysis

Mean differences between experimental groups were determined by student *t*-test or one-way analysis of variance (ANOVA) followed by a Bonferroni post-hoc test. Differences were considered statistically significant at $p < 0.05$.

Abbreviations

PD Parkinson's Disease

UA Uric acid

IMP Inosine 5'-monophosphate

MPTP 1-methyl-4-phenyl-1,2,3,6-tetrahydropyridine

SVZ Subventricular zone

BrdU Bromodeoxyuridine

MPP^+ 1-methyl-4-phenylpyridinium

NPC Neural precursor cell

NSC Neural stem cell

SN Substantia nigra

ROS Reactive oxygen species

KOx Oxonate potassium

RMS Rostral migratory stream

TH Tyrosine hydroxylase

Declarations

Author contributions

J.E.L: Writing draft, Performing experiments; Y.J.S, H.N.K, D.Y.K, S.J.C, H.S.Y: Data discussion; J.Y.S: Technical support, Supervision, Data discussion, Correcting draft; P.H.L: Data discussion, Writing-Review & Editing draft, Supervision, Funding acquisition

Funding

This research was supported by the Basic Science Research Program through the National Research Foundation of Korea (NRF) funded by the Ministry of Science, ICT and Future Planning (grant number: NRF-2019R1A2C2085462) and the Brain Korea 21 PLUS Project for Medical Science, Yonsei University.

Competing interests

The authors declare no competing interests.

References

1. Berdugo-Vega, G. *et al.* Increasing neurogenesis refines hippocampal activity rejuvenating navigational learning strategies and contextual memory throughout life. *Nature communications* **11**, 135. (2020).

2. Scopa, C. *et al.* Impaired adult neurogenesis is an early event in Alzheimer's disease neurodegeneration, mediated by intracellular Abeta oligomers. *Cell Death Differ* **27**, 934-948. (2020).

3. Winner, B. & Winkler, J. Adult neurogenesis in neurodegenerative diseases. *Cold Spring Harbor perspectives in biology* **7**, a021287. (2015).

4. Gil-Mohapel, J., Simpson, J. M., Ghilan, M. & Christie, B. R. Neurogenesis in Huntington's disease: can studying adult neurogenesis lead to the development of new therapeutic strategies? *Brain Res* **1406**, 84-105. (2011).

5. Luo, L. & O'Leary, D. D. Axon retraction and degeneration in development and disease. *Annual review of neuroscience* **28**, 127-156. (2005).

6. Geraerts, M., Krylyshkina, O., Debyser, Z. & Baekelandt, V. Concise review: therapeutic strategies for Parkinson disease based on the modulation of adult neurogenesis. *Stem Cells* **25**, 263-270. (2007).

7. Jankovic, J. Parkinson's disease and movement disorders: moving forward. *The Lancet. Neurology* **7**, 9-11. (2008).

8. Hwang, O. Role of oxidative stress in Parkinson's disease. *Exp Neurobiol* **22**, 11-17. (2013).

9. Squadrito, G. L. *et al.* Reaction of uric acid with peroxynitrite and implications for the mechanism of neuroprotection by uric acid. *Arch Biochem Biophys* **376**, 333-337. (2000).

10. Tana, C., Ticinesi, A., Prati, B., Nouvenne, A. & Meschi, T. Uric Acid and Cognitive Function in Older Individuals. *Nutrients* **10**. (2018).

11. Wen, M. *et al.* Serum uric acid levels in patients with Parkinson's disease: A meta-analysis. *PloS one* **12**, e0173731. (2017).

12. Bakshi, R. *et al.* Urate mitigates oxidative stress and motor neuron toxicity of astrocytes derived from ALS-linked SOD1(G93A) mutant mice. *Molecular and cellular neurosciences* **92**, 12-16. (2018).

13. Scheepers, L. *et al.* Urate and risk of Alzheimer's disease and vascular dementia: A population-based study. *Alzheimers Dement* **15**, 754-763. (2019).

14. Auinger, P., Kieburtz, K. & McDermott, M. P. The relationship between uric acid levels and Huntington's disease progression. *Movement disorders : official journal of the Movement Disorder Society* **25**, 224-228. (2010).

15. Li, X. *et al.* Effect of serum uric acid on cognition in patients with idiopathic REM sleep behavior disorder. *Journal of neural transmission (Vienna, Austria : 1996)* **125**, 1805-1812. (2018).

16. Ya, B. L. *et al.* Uric Acid Protects against Focal Cerebral Ischemia/Reperfusion-Induced Oxidative Stress via Activating Nrf2 and Regulating Neurotrophic Factor Expression. *Oxidative medicine and cellular longevity* **2018**, 6069150. (2018).

17. Beckervordersandforth, R. Mitochondrial Metabolism-Mediated Regulation of Adult Neurogenesis. *Brain plasticity (Amsterdam, Netherlands)* **3**, 73-87. (2017).

18. Zheng, H. *et al.* Mitochondrial oxidation of the carbohydrate fuel is required for neural precursor/stem cell function and postnatal cerebellar development. *Sci Adv* **4**, eaat2681. (2018).

19. Khacho, M. *et al.* Mitochondrial Dynamics Impacts Stem Cell Identity and Fate Decisions by Regulating a Nuclear Transcriptional Program. *Cell stem cell* **19**, 232-247. (2016).

20. Khacho, M. *et al.* Mitochondrial dysfunction underlies cognitive defects as a result of neural stem cell depletion and impaired neurogenesis. *Human molecular genetics* **26**, 3327-3341. (2017).

21. Hollenbeck, P. J. & Saxton, W. M. The axonal transport of mitochondria. *Journal of cell science* **118**, 5411-5419. (2005).

22. Okamoto, K. & Shaw, J. M. Mitochondrial morphology and dynamics in yeast and multicellular eukaryotes. *Annual review of genetics* **39**, 503-536. (2005).

23. Beckervordersandforth, R. *et al.* Role of Mitochondrial Metabolism in the Control of Early Lineage Progression and Aging Phenotypes in Adult Hippocampal Neurogenesis. *Neuron* **93**, 560-573.e566. (2017).

24. Khacho, M. & Slack, R. S. Mitochondrial dynamics in the regulation of neurogenesis: From development to the adult brain. *Developmental dynamics : an official publication of the American Association of Anatomists* **247**, 47-53. (2018).

25. Arrázola, M. S. *et al.* Mitochondria in Developmental and Adult Neurogenesis. *Neurotox Res* **36**, 257-267. (2019).

26. Flippo, K. H. & Strack, S. Mitochondrial dynamics in neuronal injury, development and plasticity. *Journal of cell science* **130**, 671-681. (2017).

27. Kuhn, H. G., Eisch, A. J., Spalding, K. & Peterson, D. A. Detection and Phenotypic Characterization of Adult Neurogenesis. *Cold Spring Harbor perspectives in biology* **8**, a025981. (2016).

28. Mishra, A., Singh, S., Tiwari, V., Parul & Shukla, S. Dopamine D1 receptor activation improves adult hippocampal neurogenesis and exerts anxiolytic and antidepressant-like effect via activation of Wnt/beta-catenin pathways in rat model of Parkinson's disease. *Neurochem Int* **122**, 170-186. (2019).

29. Winner, B. *et al.* Role of alpha-synuclein in adult neurogenesis and neuronal maturation in the dentate gyrus. *J Neurosci* **32**, 16906-16916. (2012).

30. Winner, B. *et al.* Human wild-type alpha-synuclein impairs neurogenesis. *J Neuropathol Exp Neurol* **63**, 1155-1166. (2004).

31. Winner, B. *et al.* Mutant alpha-synuclein exacerbates age-related decrease of neurogenesis. *Neurobiol Aging* **29**, 913-925. (2008).

32. Crews, L. *et al.* Alpha-synuclein alters Notch-1 expression and neurogenesis in mouse embryonic stem cells and in the hippocampus of transgenic mice. *J Neurosci* **28**, 4250-4260. (2008).

33. Kohl, Z. *et al.* Fluoxetine rescues impaired hippocampal neurogenesis in a transgenic A53T synuclein mouse model. *Eur J Neurosci* **35**, 10-19. (2012).

34. Valenti, D. *et al.* Inhibition of Drp1-mediated mitochondrial fission improves mitochondrial dynamics and bioenergetics stimulating neurogenesis in hippocampal progenitor cells from a Down syndrome mouse model. *Biochim Biophys Acta Mol Basis Dis* **1863**, 3117-3127. (2017).

35. de Lau, L. M., Koudstaal, P. J., Hofman, A. & Breteler, M. M. Serum uric acid levels and the risk of Parkinson disease. *Annals of neurology* **58**, 797-800. (2005).

36. Euser, S. M., Hofman, A., Westendorp, R. G. & Breteler, M. M. Serum uric acid and cognitive function and dementia. *Brain : a journal of neurology* **132**, 377-382. (2009).

37. Huang, T. T., Hao, D. L., Wu, B. N., Mao, L. L. & Zhang, J. Uric acid demonstrates neuroprotective effect on Parkinson's disease mice through Nrf2-ARE signaling pathway. *Biochemical and biophysical research communications* **493**, 1443-1449. (2017).

38. Ni, H. M., Williams, J. A. & Ding, W. X. Mitochondrial dynamics and mitochondrial quality control. *Redox Biol* **4**, 6-13. (2015).

39. Yuan, T. F., Gu, S., Shan, C., Marchado, S. & Arias-Carrion, O. Oxidative Stress and Adult Neurogenesis. *Stem Cell Rev Rep* **11**, 706-709. (2015).

40. Kopin, I. J. MPTP: an industrial chemical and contaminant of illicit narcotics stimulates a new era in research on Parkinson's disease. *Environ Health Perspect* **75**, 45-51. (1987).

41. Banerjee, K. *et al.* Alpha-synuclein induced membrane depolarization and loss of phosphorylation capacity of isolated rat brain mitochondria: implications in Parkinson's disease. *FEBS Lett* **584**, 1571-1576. (2010).

42. Melo, T. Q., Copray, S. & Ferrari, M. F. R. Alpha-Synuclein Toxicity on Protein Quality Control, Mitochondria and Endoplasmic Reticulum. *Neurochem Res* **43**, 2212-2223. (2018).

43. Mishra, A. *et al.* Dopamine receptor activation mitigates mitochondrial dysfunction and oxidative stress to enhance dopaminergic neurogenesis in 6-OHDA lesioned rats: A role of Wnt signalling. *Neurochem Int* **129**, 104463. (2019).

44. Hoglinger, G. U. *et al.* Dopamine depletion impairs precursor cell proliferation in Parkinson disease. *Nature neuroscience* **7**, 726-735. (2004).

45. Winner, B. *et al.* Dopamine receptor activation promotes adult neurogenesis in an acute Parkinson model. *Exp Neurol* **219**, 543-552. (2009).

46. O'Sullivan, S. S. *et al.* The effect of drug treatment on neurogenesis in Parkinson's disease. *Movement disorders : official journal of the Movement Disorder Society* **26**, 45-50. (2011).

47. O'Reilly, E. J. *et al.* Plasma urate and Parkinson's disease in women. *American journal of epidemiology* **172**, 666-670. (2010).

48. Na Kim, H. *et al.* Feasibility and Efficacy of Intra-Arterial Administration of Mesenchymal Stem Cells in an Animal Model of Double Toxin-Induced Multiple System Atrophy. *Stem Cells Transl Med* **6**, 1424-1433. (2017).

49. Oh, S. H., Kim, H. N., Park, H. J., Shin, J. Y. & Lee, P. H. Mesenchymal Stem Cells Increase Hippocampal Neurogenesis and Neuronal Differentiation by Enhancing the Wnt Signaling Pathway in an Alzheimer's Disease Model. *Cell Transplant* **24**, 1097-1109. (2015).

50. Kim, H. N., Shin, J. Y., Kim, D. Y., Lee, J. E. & Lee, P. H. Priming mesenchymal stem cells with uric acid enhances neuroprotective properties in parkinsonian models. *J Tissue Eng* **12**, 20417314211004816. (2021).

Figures

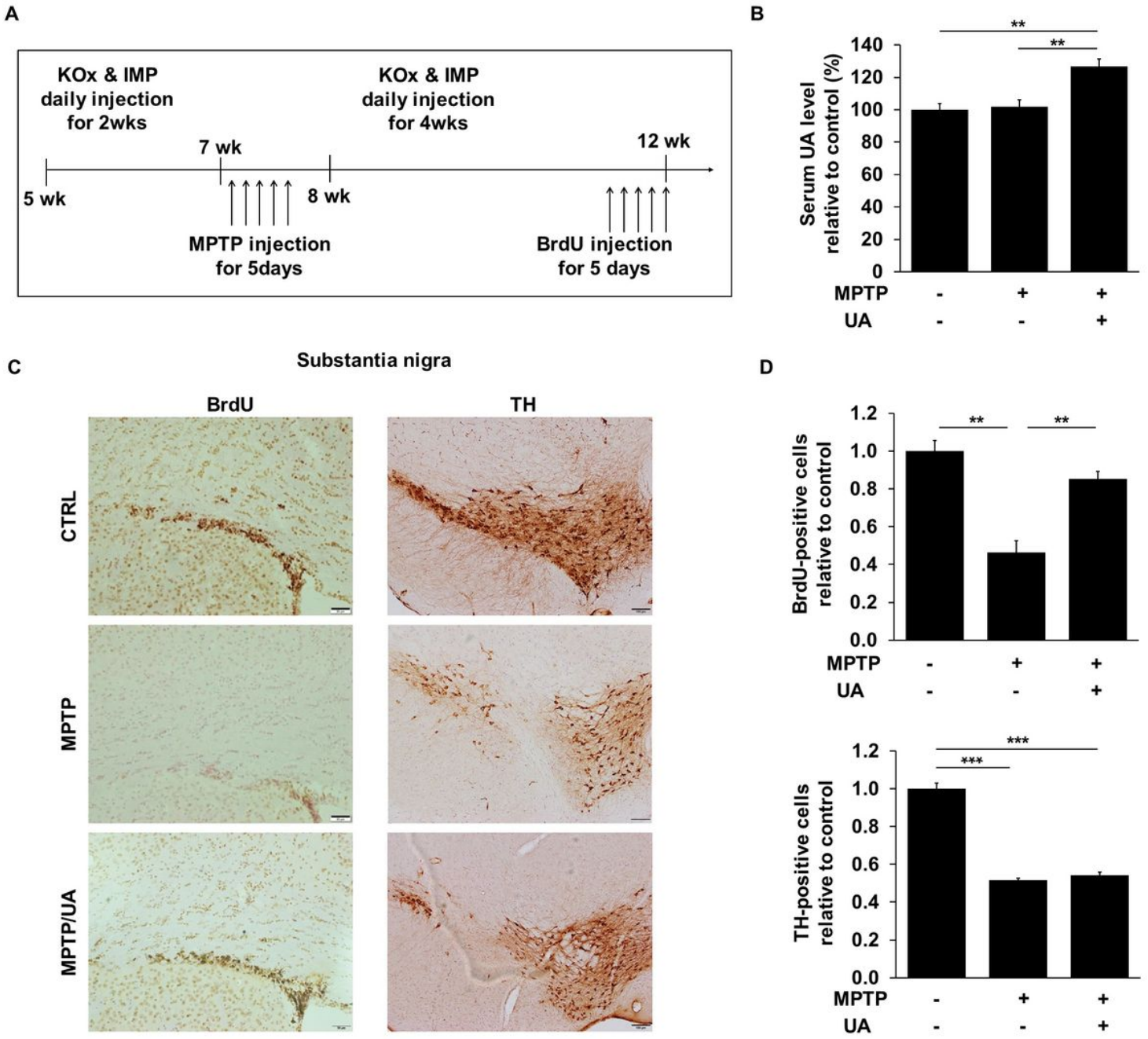

Figure 1

UA elevation increased the number of BrdU-positive cells in the SVZ of a MPTP-induced PD animal model. (A): Animal experimental schedule design. (B): Serum UA levels were significantly higher in mice that received IMP with KOx as compared to control and MPTP-treated mice (n = 8 per group). (C, D): The number of BrdU-positive cells in SVZ at 12 weeks. PD mice with high serum UA levels showed considerably more BrdU-positive cells as compared to either PD mice with normal serum UA levels or control mice (n = 5 per group). The number of TH-positive cells in the SN at 12 weeks. Both PD mice with high and normal UA levels revealed a significant reduction in the number of TH-positive cells compared to the control group. There was no statistically significant difference between PD mice with high serum UA

levels and those with normal levels (n = 5 per group). The data are presented as mean ± SE. *p<0.05, **p<0.01 and ***p<0.001

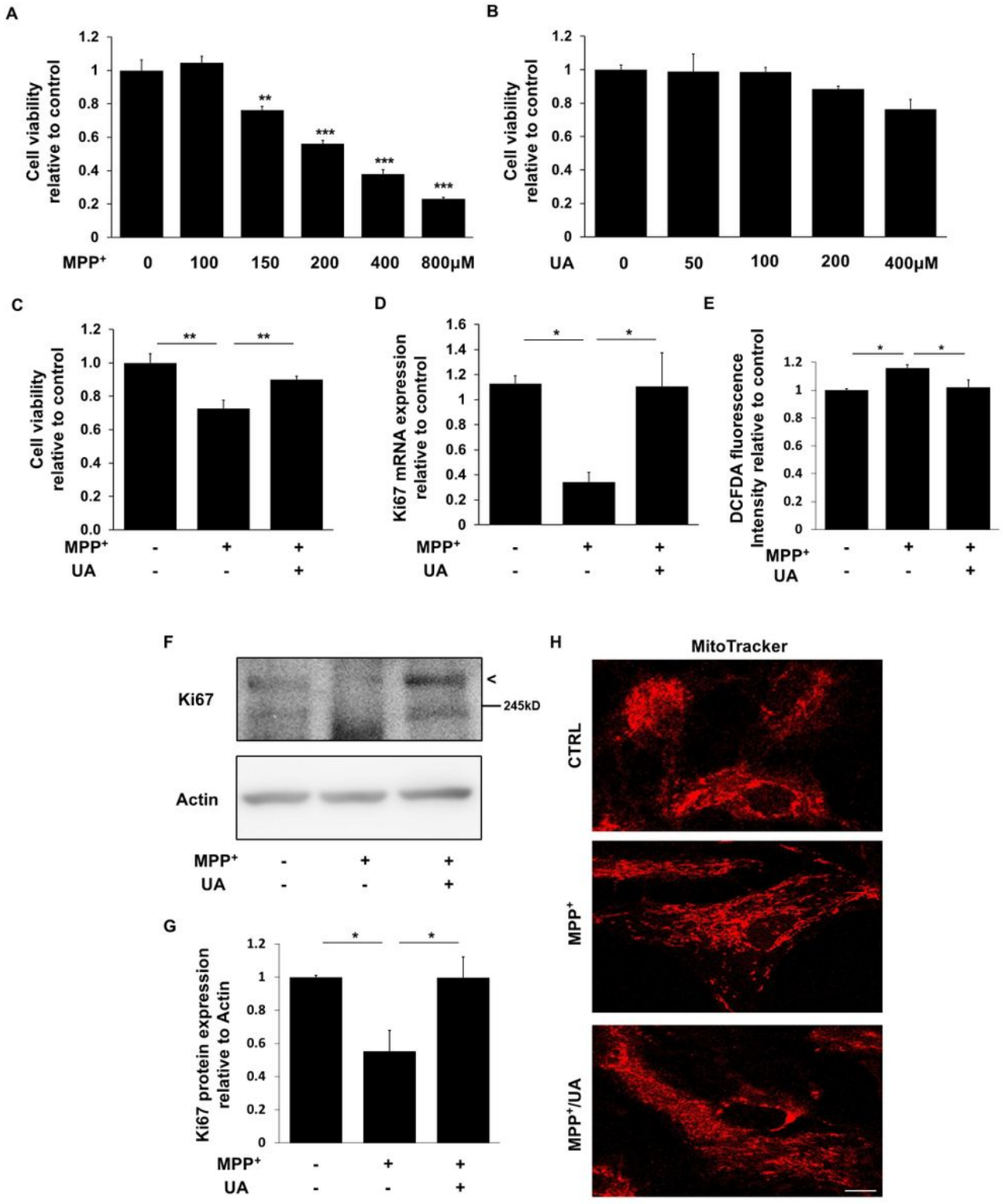

Figure 2

UA treatment exerted neuroprotective effect and promoted proliferation in primary cultured NPCs. (A): MTS analysis in MPP+-treated NPCs with a concentration of 100, 150, 200, 400, and 800 μM. 150 μM of MPP+ treatment induced about 56% of viability on NPCs (n = 4 per group). (B): MTS analysis in UA-

treated NPCs with a concentration of 50, 100, 200, and 400 μM. UA treatment did not induce statistically significant cell death up to 400 μM (n = 4 per group). (C): MTS analysis in MPP+ treated or MPP+ with UA-treated NPCs at a 150 μM concentration of UA for 24 h and MPP+ for 72 h with UA co-treatment. UA exerted a neuroprotective effect on NPCs by restoring cell viability up to 90% compared to control (n = 4 per group). (D): Quantitative RT-PCR for proliferation marker, Ki67. The expression level of Ki67 was reduced to 41.6%; however, UA restored it to 92.2% compared to control. (E): Intracellular ROS as measured by DCFDA assay after MPP+ and UA treatment. MPP+-induced ROS was scavenged by UA pre-treament. (F): Western blot for proliferation marker, Ki67 in MPP+ and UA-treated NPCs. (G): Quantification graph of Ki67 western blot analysis. (H) Immunofluorescent labeling for mitotracker. MPP+-treated NPCs showed fragmented mitochondrial morphology, whereas UA treatment restored them similar to those of controls. Scale bar: 10μm. The data are presented as the mean ± SE. *p<0.05, **p<0.01 and ***p<0.001

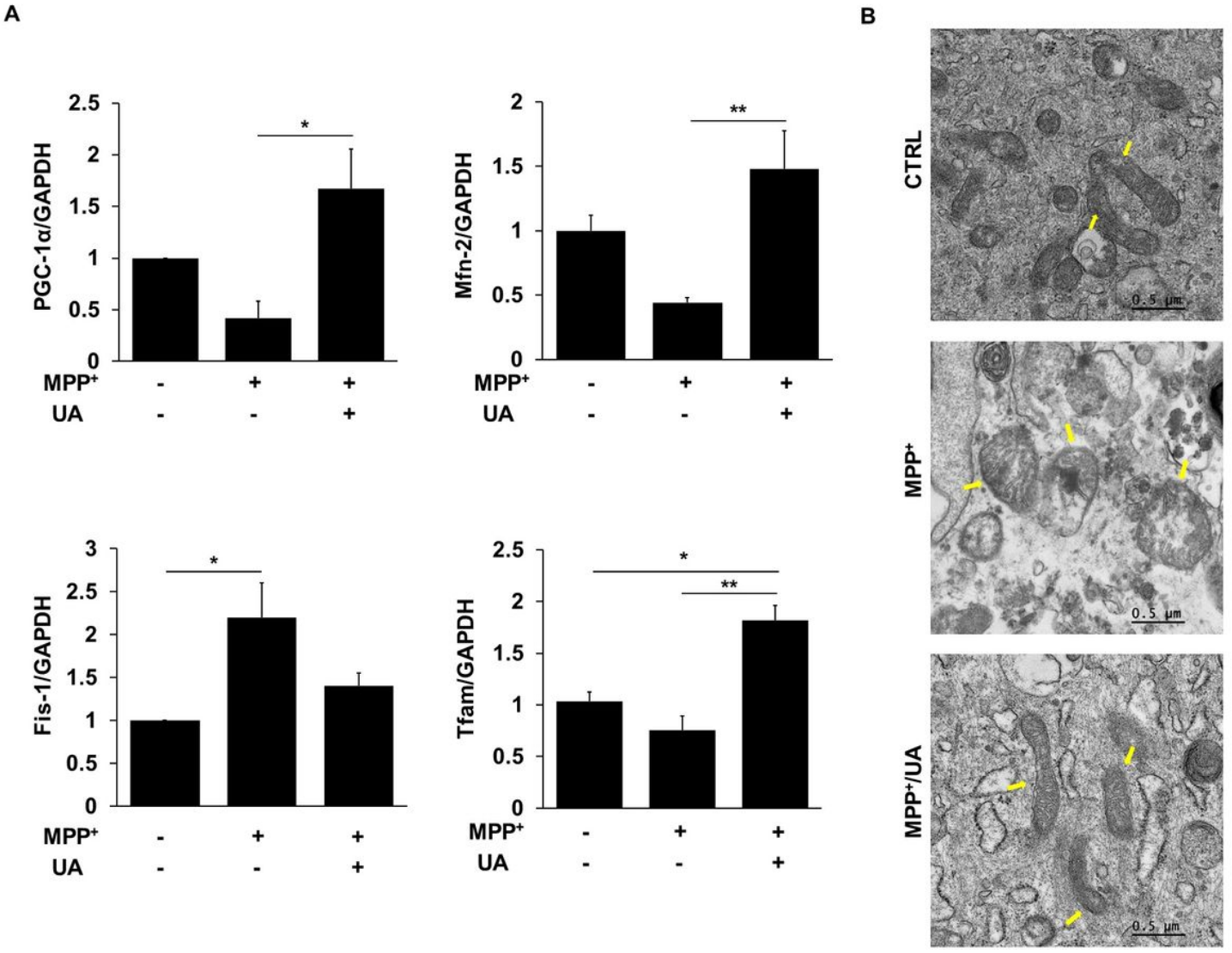

Figure 3

UA treatment rescued the mitochondrial phenotype via modulating mitochondrial dynamics in NPCs. (A): Quantitative RT-PCR for mitochondria master regulator, PGC-1α, mitochondrial fission marker, Fis1,

mitochondrial fusion marker, Mfn2, and mitochondrial transcription factor, Tfam. MPP+ treatment led to a significant decrease in the expression level of PGC-1α, Mfn2, and Tfam and UA treatment has restored it. On the contrary, the expression level of Fis1 was increased when exposed to MPP+-, and UA treatment restored it (n = 5 per group). (B): TEM analysis revealed that MPP+ treatment induced severe abnormal morphology of mitochondria with a swollen body and fragmented phenotype. However, UA treatment returned mitochondria morphology to a similar state as control NPCs. The arrows indicate mitochondria. The data are presented as mean ± SE. *p<0.05, **p<0.01 and ***p<0.001

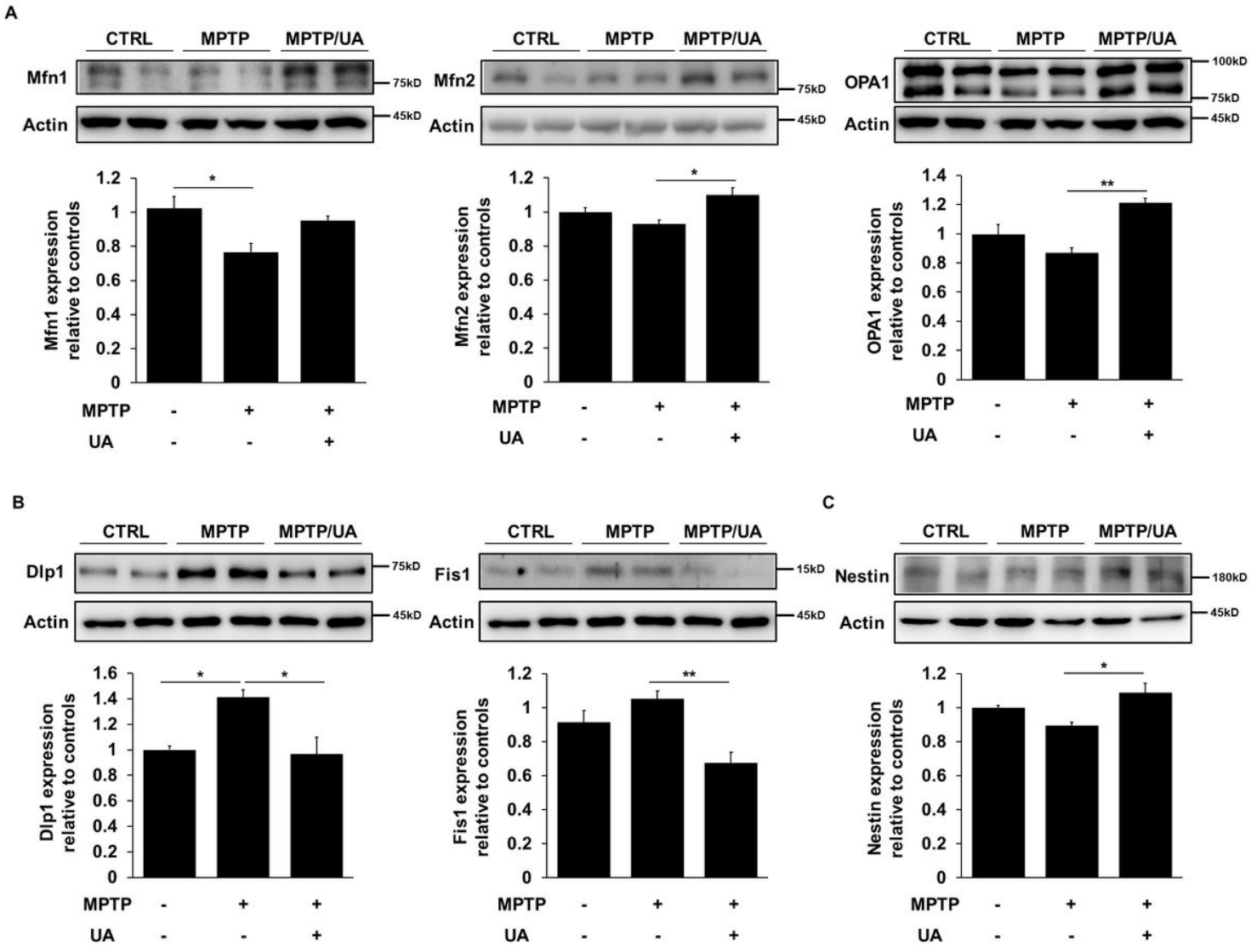

Figure 4

PD mice with high serum UA level showed modulated mitochondrial dynamics. (A): Western blot for mitochondrial fusion markers, Mfn1, Mfn2, and Opa1. The expression levels of Mfn1, Mfn2, and OPA1 were decreased in PD mice and upregulated in UA-elevated PD mice (n = 5 per group). (B): Western blot for mitochondrial fission markers, Dlp and Fis1. The expression levels of Dlp and Fis1 were increased in

PD mice and significantly suppressed in PD mice with high serum UA levels (n = 5 per group). (C): Western blot for neural stem cell marker, nestin. The expression levels of nestin were significantly increased in UA-elevated PD mice compared to control or PD mice with normal UA levels (n = 5 per group). The data are presented as mean ± SE. *p<0.05, **<0.01 and ***p<0.001

Supplementary Files

This is a list of supplementary files associated with this preprint. Click to download.

- Supplementarydata.docx
- Supplementaryinformation.pdf